

## Estimation of Parameters of the Rail Corrugation

George TUMANISHVILI<sup>1</sup>, Tamaz NATRIASHVILI<sup>2</sup>, Tengiz NADIRADZE<sup>3</sup>, Giorgi TUMANISHVILI<sup>4</sup>

<sup>1-4</sup>Department of Machine dynamics, Institute of Machine Mechanics, Georgia

### ABSTRACT

A characteristic roll-slip phenomenon between the wheel and the rail are prone to develop a wavy wear of the railhead surface, known as rail rutting corrugation. There are a lot of scientific works and various opinions about destruction of interacting surfaces of wheels and rails, including the rutting wear of rails, but some aspects of this phenomena are still insufficiently studied.

The influence of a difference of the ways passed by wheels of the wheel-set at its movement in curves, at Movement of the wheel-set with the wheels of different diameters in the straight track and at Movement of the wheel-set with one wheel having ellipticity in the straight track on the periodic twisting of the wheel-set shaft is considered in the work. A sliding distance at slipping of the tread surface on a rail caused by the periodic untwisting of the extremely twisted axis of the wheel-set and emergence of the wave wear of rails are estimated. Sharp change of the friction forces is considered as a result of destruction of the third body and the beginning of emergence of the heaviest type of wear - scuffing. The friction control, decrease of the power and thermal loading and providing the steady third body in the contact zone are considered as the main directions for decreasing and avoiding the rutting corrugation.

**Keywords:** rail; corrugation; slip; wheel; wear.

### I. INTRODUCTION

The development of periodic irregularities with distinct wavelengths (corrugation) on the low rail of small radius curves leads to rise to noise, ground-borne vibration and more general dynamic loading, which increases damage of components of both vehicle and track; Corrugation can also generate rolling contact fatigue (RCF), such as squats [1]. It commonly observed in all types of railway tracks and is studied during of long time [2-4]. There are many scientific works, devoted to this subject, but some aspects of this problem remain unsolved until today [1, 4], that complicate the prevention of undesirable phenomena produced them and leads the hard-economic problems. The most common 'damage mechanism' on almost all types of railways is wear [5]. In Europe, corrugation treatment and control remain the main reason for expensive rail grinding on all railway systems [6]. The longitudinal vibration is probably dominant for short pitch corrugation initiation [7]; Classification of the ratcheting wear be of the form according to S. L. Grassie shown that the ratcheting wear can take place in both the straights and curves. Creation of wave profile on the tread surface of the rail is possible by various reasons.

### II. PECULIARITIES OF THE WHEEL-SET MOVEMENT

In the straight a wheel-set performs a zigzag movement close to the sinusoid which is accompanied by creeping. In curves, the inner wheel passes the shorter distance which causes deviation of the wheel set axis from radial disposition.

It leads to increase of the angle of attack, lateral force and rolling resistance of outer wheel of the front wheel-set of the bogie and promotes problems of wheel-flange climb derailment, squealing noise, thin flange wear of the wheel, gauge face wear of high-rail and corrugations basically of the low-rail. In such conditions, to return the wheel-set into initial position it is necessary that one of the wheel of the wheel-set slide on the rail in the longitudinal direction. There are a lot of attempts to obtain of the wheel-set more or less radial position [8, 9].

The tread surface of the wheel is conical and is gradually passing into flange surface through flange root. Therefore, the differences between diameters of interacting surfaces inside of the contact zone, relative sliding, contact stresses, deformations and temperatures towards the flange are growing. The raised power and thermal loading provokes destruction of the third body and uncontrolled deterioration of interacting surfaces. In the such conditions, the surfaces become more sensitive to the area of actual contact and of the amount of the interacting roughness. So, for the heavy loaded surfaces the friction forces depend on the size of contact zone. In operation, the initial bounded contact area is growing because of wear and for worn profiles of wheels and rails they will be considerably greater. Increasing the friction force on the flange surface and decreasing the angle of inclination of the flange will promotes the wheels to climb onto the top of the rail head and then derail. The movement of the wheel-set in the curve commonly leads to periodical advancing of the inner wheel relative to the outer wheel and the further return of the symmetry axis of wheel-set near initial position by sliding of a wheel on a rail that is the cause of periodic torsion deformations of an axis of a wheel-set and wear of the wheel and rail. The intermittent slipping of one of the wheel of the wheel-set can produces the torsional vibrations of the wheel-set and the longitudinal vibrations of the vehicle (that have been identified as flange noise [10]) and the respective wear of wheels and rails, like to corrugation. In the Fig. 1 is shown the movement of a wheel-set on the track in the curve and a corrugated inner rail.

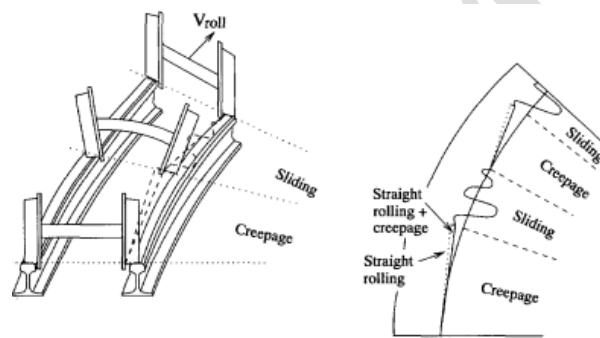


Fig. 1. Movement of a wheel-set on the track in the curve and a corrugated inner rail [11].

The similar picture would be at various diameters of the tread surfaces or at various brake efforts of a wheel set. The wheel-rail contact is a rolling and sliding contact, which can be divided into stick (no slip) and slip zones.

### III. ESTIMATION OF PARAMETERS OF THE RAIL CORRUGATION

We estimate parameters of the rail corrugation, distances between worn-out segments of the rail, lengths of these segments and depth of the worn-out layers caused by the three different reasons. We determine first distances between worn out segments.

- A. **Movement of the wheel-set in the curve.** At pure rolling (without sliding) of the wheel-set with velocity  $V$  in the curve of radius  $R$  through angle  $\alpha$ , the inner wheel will rotate relative to the outer wheel in the counterclockwise direction if it is seen from axial direction A (Fig.3) and it will twist the wheel-set axle through angle  $\varphi$ . This latter will be equal to the ratio of the difference  $\Delta l$  of the outer and inner arcs to the radius  $D/2$  of the wheel tread surface:

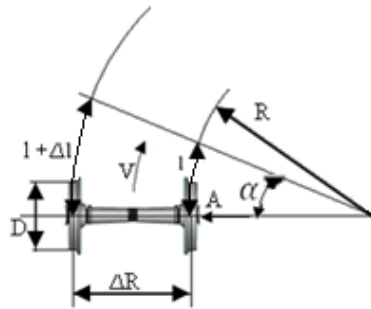


Fig.2. Movement of the wheel-set in the curve

$$\varphi = 2\Delta l/D.$$

From the drawing  $\alpha = l/R = (l+\Delta l)/(R+\Delta R) = \Delta l/\Delta R$  from where  
 $\Delta l = l\Delta R/R,$

(1)

and therefore

$$\varphi = 2l\Delta R/DR, \quad (2)$$

The maximum angle of twist of the wheel-set axle  $\varphi_{\max}$  depends on the friction force

$$F = fQ \quad (3)$$

and is calculated by the formula

$$\varphi_{\max} = ML/I_p G \quad (4)$$

where M is a torque caused by the friction force

$$M = FD/2 = fQD/2; \quad (5)$$

f – friction coefficient; Q – thrust load of the wheel on the rail; L – length of the wheel-set axle;  $I_p$  – polar moment of inertia of the wheel-set axle cross section; G – modulus of rigidity of the axle material.

We determine path l necessary for the axle to be twisted on the maximum angle  $\varphi_{\max}$  (or distance between worn out segments of the rail since at travelling this path the wheels are rolling on the rail without sliding) from (2) replacing  $\varphi$  by  $\varphi_{\max}$ :

$$l = DR \varphi_{\max} / 2\Delta R = MLDR / 2I_p G \Delta R \quad (6)$$

and putting the found l into (1) we obtain correspondingly

$$\Delta l = MLD / 2I_p G \quad (7)$$

**B. Movement of the wheel-set with the wheels of different diameters in the straight track.** At rolling of the wheel-set with the wheels of different diameters D and D+ΔD in the straight track, in the case of the same angle of rotation these wheels will pass correspondingly the distances l and l+Δl (Fig.4a).

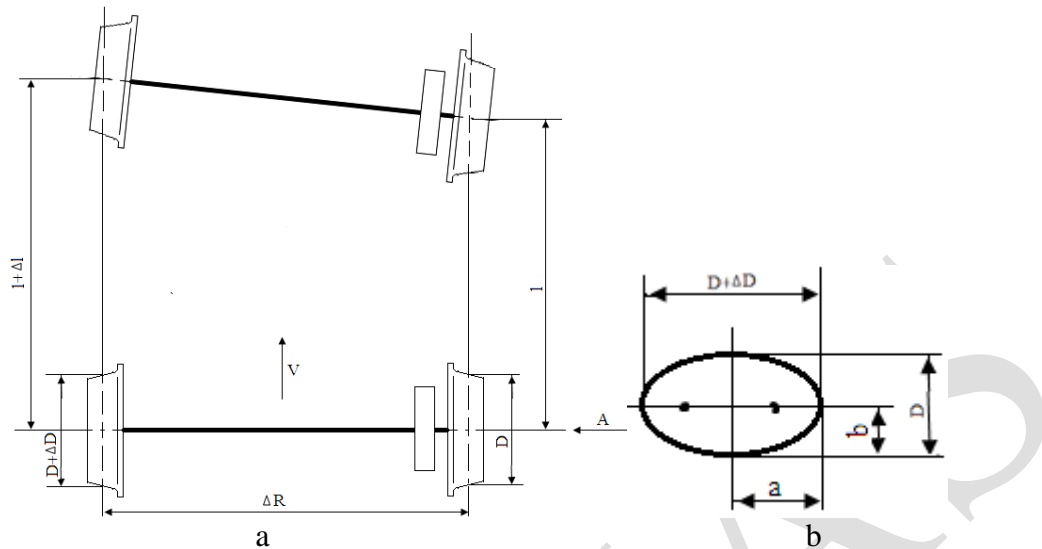


Fig.3. Movement of the wheel-set in the straight track: a) with the wheels of different diameters or with one wheel having ellipticity; b) parameters of ellipticity.

At rolling of the smaller wheel through distance  $l$  it will rotate relative to the bigger wheel in the counterclockwise direction if it is seen from axial direction  $A$  and it will twist the wheel-set axle through angle  $\varphi = 2\Delta l / (D + \Delta D)$ , from where, considering the formula (4) we obtain the value of  $\Delta l$  corresponding to the maximum angle of twist  $\varphi_{\max}$  of the axle

$$\Delta l = \varphi_{\max} (D + \Delta D) / 2 = ML(D + \Delta D) / 2IpG \quad (8)$$

The following proportion can be written from the drawing  $(l + \Delta l) / l = (D + \Delta D) / D$  or  $\Delta l / l = \Delta D / D$ , from which we obtain distance  $l$  (distance between the worn out segments) at passing of which the wheel-set axle will be twisted through angle  $\varphi_{\max}$

$$l = \Delta l D / \Delta D = ML(D + \Delta D) D / 2IpG \Delta D \quad (9)$$

**C. Movement of the wheel-set with one wheel having ellipticity in the straight track.** Consider movement of such wheel-set in the straight track whose one wheel has a tread surface of diameter  $D$  and the other wheel has ellipticity with the small  $D$  and bigger  $D + \Delta D$  diameters (Fig. 4a).

At one revolution, these wheels will pass the different distances, correspondingly  $l$  and  $l + \Delta l$ , because of which a wheel with diameter  $D$  will rotate relative to the elliptical wheel in the counterclockwise direction when it is seen from axial direction  $A$  and it will twist the wheel-set axle through angle

$$\varphi = 2\Delta l / D_a \quad (10)$$

where average diameter of the elliptical wheel

$$D_{av} = D + \Delta D / 2 \quad (11)$$

The difference of distances passed by the wheels at one revolution is  $\Delta l = L - \pi D$ , where the length of the elliptical tread surface

$$L = \pi [3(a+b) - \sqrt{(3a+b)(a+3b)}] \quad (12)$$

or

$$\Delta l = \pi [3(a+b) - \sqrt{(3a+b)(a+3b)}] - \pi D \quad (13)$$

The value  $\Delta l^I$  corresponding to maximum angle of twist  $\phi_{max}$  of the axle is obtained from (10)

$$\Delta l^I = \phi_{max} D_{av} / 2 = ML(D + \Delta D / 2) / 2I_p G \quad (14)$$

The distance  $l$  at passing of which the wheel-set axle will be twisted on the angle  $\phi_{max}$

$$l = \pi D \Delta l^I / \Delta l \quad (15)$$

In all the three cases considered above at removing or decrease of the torque  $M$  acting on the wheel that takes place at its vertical vibrations when the friction force  $F$  decreases, the angle of twist of the axle will start to decrease. Suppose  $\phi_{max}$  falls down to zero during time  $t$ . This will take place at rotation of the inner wheel in the clockwise direction relative to the outer wheel on the angle  $\phi_{max}$  since the flange of the outer wheel is pressed on the rail and its movement is additionally restricted by the friction force arisen between the flange and rail. Obviously, during this time  $t$  the inner wheel will roll and slide simultaneously on the rail and the rolling and sliding distance on the rail will be

$$S_r = Vt \quad (16)$$

We note that the rolling and sliding distance on the wheel tread surface is  $S_w = \Delta l + S_r$  or  $S_w = \Delta l^I + S_r$  for the variant C (17)

where  $\Delta l$  or  $\Delta l^I$  is a sliding friction path and the wave length of the worn-out rail (Fig.5)

$$W = l + S_r \quad (18)$$

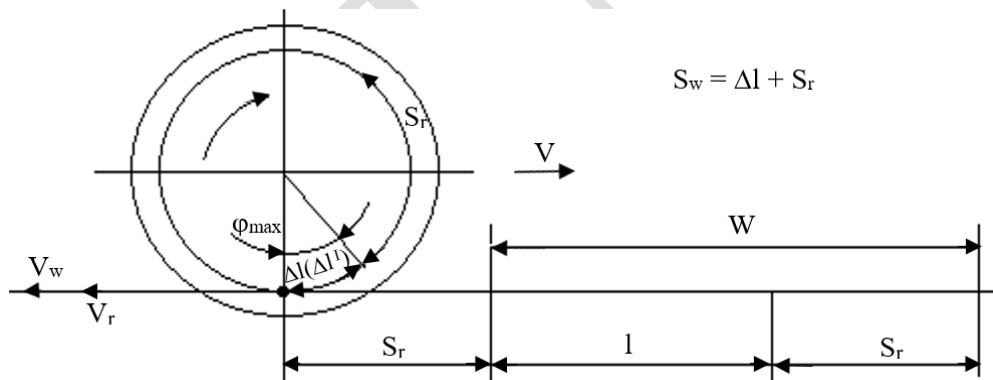


Fig.4. The rolling and sliding distances on the rail and wheel.

This value of the wave length assumes that at release of the inner wheel the friction force acting on it from the rail is zero. When the friction force differs from zero the wave length will be less since its both components will be decreased and its value depends on the friction force magnitude.

To determine time  $t$  we present the wheel-set as a one-mass torsion vibratory system (Fig. 6a), where  $C$  is the torsion rigidity of the wheel-set axle,  $I$  – total moment of inertia of the inner wheel and gear wheel located near it. Then, angle of twist  $\phi_{max}$  will fall down to zero in conformity with a law of free vibrations of this vibratory system during the period  $P/4$  (Fig. 6b).

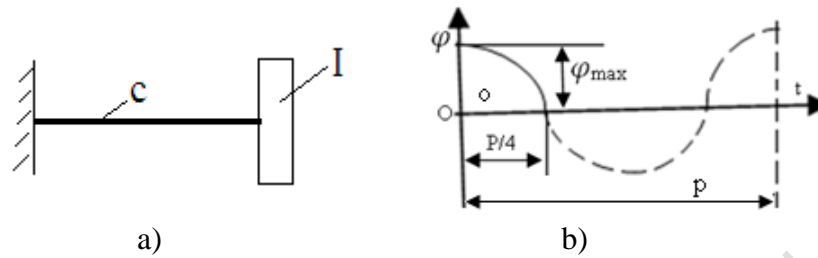


Fig.5. a) One-mass torsion vibratory system; b) Graph of the system free vibrations.

At that, period of free vibrations

$$P = 2\pi\sqrt{I/C} \quad (19)$$

and consequently time  $t$  will be

$$t = P/4 = \frac{\pi}{2}\sqrt{I/C} \quad (20)$$

The average velocity of the wheel contact point relative to the wheel center (Fig.5)

$$V_w = -\frac{D\varphi_{\max}}{2t} + V_r \quad (21)$$

where  $V_r = -V$  is a velocity of the rail contact point relative to the wheel center.

We note that maximum velocity of the wheel contact point relative to the wheel center

$$V_w^I = -\frac{A\omega D}{2} + V_r = -\varphi_{\max}\sqrt{\frac{C}{I}} \times \frac{D}{2} + V_r \quad (21^I)$$

where  $A = \varphi_{\max}$  is an amplitude of the wheel-set shaft torsion vibrations;

$\omega = \sqrt{C/I}$  - cyclic frequency of vibrations.

$$\text{Sliding velocity } V_{sl} = V_w - V_r \quad (22)$$

Relative sliding velocities for the rail and wheel

$$K_r = \frac{V_{sl}}{V_r} \times 100\% \quad \text{and} \quad K_w = \frac{V_{sl}}{V_w} \times 100\% \quad (23)$$

The depth of the worn-out layer a year of the rail segment  $S_r$

$$h = i\Delta N \quad (24)$$

where  $i$  is the wear intensity and  $N$  – number of cycles which is determined as follows

$$N = N_1 N_2 N_3 N_4 \quad (25)$$

where  $N_1$  is a number of the trains passing by a day;  $N_2$  – number of wagons in the train;  $N_3$  – number of wheels on one side of the wagon;  $N_4$  – number of days a year.

**Numerical calculation** is carried out for the locomotive wheel-set with the following parameters:

$$D = 1250 \text{ mm}; \Delta D = 3 \text{ mm}; L = 1580 \text{ mm}; I_p = 1.57 \times 10^{-4} \text{ m}^4; G = 75 \text{ GPa}; Q = 115 \text{ KN}; I = 176 \text{ kgm}^2; C = 7450 \text{ KNm}; f = 0.4; \Delta R = 1546 \text{ mm}.$$

$$\text{The torque } M = fQD/2 = 0.4 \times 115 \times 1.25/2 = 28.75 \text{ KNm};$$

Maximum angle of twist of the axle

$$\varphi_{\max} = ML/I_p G = (28.75 \times 10^3 \times 1.58) / (1.57 \times 10^{-4} \times 75 \times 10^9) = 0.00386 \text{ rad} = 0.221^\circ;$$

Determine first distances  $l$  between the worn out segments for the considered cases:

a) On the base of (6) we have:

$$\text{For } R=200 \text{ m}; \quad l = DR \varphi_{\max} / 2\Delta R = (1.25 \times 200 \times 0.00386) / (2 \times 1.546) = 0.312 \text{ m} = 312 \text{ mm};$$

$$R = 400 \text{ m}; \quad l = 624 \text{ mm};$$

$$R = 600 \text{ m}; \quad l = 936 \text{ mm};$$

Putting the found  $l$  into (1) we obtain the same result for all the  $R$

$$\Delta l = l \Delta R / R = (0.312 \times 1.546) / 200 = 0.00241 \text{ m} = 2.412 \text{ mm};$$

b) On the base of (8) we have

$$\Delta l = ML(D + \Delta D) / 2IpG = (28.75 \times 10^3 \times 1.58)(1.25 + 0.003) / 2 \times 1.57 \times 10^4 \times 75 \times 10^9 = 2.417 \text{ mm};$$

Distance  $l$  on the base of (9) will be

$$l = \Delta l D / \Delta D = 2.417 \times 1250 / 3 = 1007.1 \text{ mm};$$

c) Semi-axes of the ellipse on the base of Fig.4b will be

$$a = (D + \Delta D) / 2 = (1250 + 3) / 2 = 626.5 \text{ mm}; \quad b = D / 2 = 1250 / 2 = 625 \text{ mm};$$

Difference of the paths travelled by the wheels at one revolution on the base of (13) will be

$$\Delta l = \pi [3(a+b) - \sqrt{(3a+b)(a+3b)}] - \pi D = 3.14 [3(626.5+625) - \sqrt{(3 \times 626.5 + 625)(626.5 + 3 \times 625)}] - 3.14 \times 1250 = 4.71 \text{ mm};$$

The value of  $\Delta l^I$  corresponding to the angle of twist  $\varphi_{\max}$  of the axle on the base of (14) will be

$$\Delta l^I = ML(D + \Delta D / 2) / 2IpG = (28.75 \times 10^3 \times 1.58)(1.25 + 0.003 / 2) / 2 \times 1.57 \times 10^4 \times 75 \times 10^9 = 2.414 \text{ mm}.$$

Distance  $l$  on the base of (15) will be

$$l = \pi D \Delta l^I / \Delta l = 3.14 \times 1250 \times 2.414 / 4.71 = 2012.7 \text{ mm}.$$

Period of the free vibrations for all the three cases considered above on the base of (19) will be

$$P = 2\pi \sqrt{\frac{l}{c}} = 2 \times 3.14 \sqrt{\frac{176}{7450 \times 10^3}} = 0.03 \text{ s};$$

Time of the simultaneous rolling and sliding according to (20) will be

$$t = P / 4 = 0.03 / 4 = 0.0075 \text{ s}.$$

The parameters  $S_r$ ,  $S_w$ ,  $V_w$ ,  $V_w^I$ ,  $V_{sl}$ ,  $K_r$  and  $K_w$  calculated according to expressions (16), (17), (21), (21<sup>I</sup>), (22) and (23) correspondingly are the same for all the three variants a), b) and c) since  $\Delta l$  is practically the same for these variants and the results for the three different velocities  $V$  are given in the table 1:

TABLE 1  
CALCULATED PARAMETERS

Velocity $V$	$S_r$ , mm	$S_w$ , mm	$V_w$ , m/s	$V_w^I$ , m/s	$V_{sl}$ , m/s	$K_r$ , %	$K_w$ , %
30 km/h=8.33 m/s	62.5	64.9	-8.65	-8.83	-0.32	3.84	3.70
50 km/h=13.88 m/s	104.1	106.5	-14.2	-14.38	-0.32	2.30	2.25
80 km/h=22.22 m/s	166.6	169.0	-22.54	-22.72	-0.32	1.44	1.40

As for the wave length  $W$  its values calculated according to (18) under supposition that to radii of curvature  $R=200, 400, 600$  m of variant a) correspond successively velocities  $V=30, 50$  and  $80$  km/h and to variants b) and c) corresponds velocity  $V=80$  km/h, are given below:

- a) For  $R=200$  m;  $W=1+ S_r =312+62.5=374.5$  mm;  
 $R=400$  m;  $W=624+104.1= 728.1$  mm;  
 $R=600$  m;  $W=936+166.6=1102.6$  mm.
- b)  $W=1007.1+166.6= 1173.7$  mm;
- c)  $W=2012.7+166.6=2179.3$  mm.

Depth of the worn-out layer on the rail segment  $S_r$  according to (24) and (25) will be

$$h= i\Delta l N_1 N_2 N_3 N_4 = 10^{-6} \times 2.4 \times 30 \times 20 \times 4 \times 365 = 2.1 \text{ mm,}$$

where  $i= 10^{-6}$ ;  $\Delta l=2.4$  mm;  $N_1=30$  trains;  $N_2=20$  wagons;  $N_3=4$  wheels;  $N_4=365$  days.

Though real parameters of the rail corrugation, length of the worn-out rail segment  $S_r$ , distance  $l$  between these worn out segments and depth of the worn-out layer on the rail segment  $S_r$  caused by the multiple movement with different velocities of the wheel-sets of various types, their vertical vibrations, torsion vibrations of the wheel-set axles and etc., differ more or less from the obtained numerical values, these latter display a general tendency of the wear of such type. It should also be taken into account that in reality the three considered reasons of the rail corrugation take place simultaneously with various combinations.

#### IV. CONCLUSIONS

At rolling of the wheel-set wheels on the rail when the distances travelled by them are different due to difference of the wheels tread surfaces, their ellipticity or at movement in the curves the wheel-set axle is subjected to the elastic torsion deformations under action of the friction forces. At the moments when the elastic forces can no more be increased due to the insufficient friction forces a periodic sliding of the wheel on the rail takes place. This results in the increased relative sliding velocity followed by the catastrophic wear that will cause the intensive rail corrugation. For decrease of the rail corrugation it is necessary to decrease the sliding friction path and relative sliding velocity, perfect the wheel-set design, modify the interacting surfaces and control the friction. This will allow us to increase and predict the rail life-time at normalized deepness of the worn-out layer and given wear rate.

#### REFERENCES

- [1]. Li, Z.; Zhao, X.; Esveld, C.; Dollevoet, R.; Molodova, M. An investigation into the causes of squats-correlation analysis and numerical modelling. *Wear* **2008**, 265, 1349–1355.
- [2]. E. Tassily, N. Vincent, Rail corrugations: analytical model and field tests, in: S.L. Grassie (Ed.), *Proceedings of the Third International Conference on Contact Mechanics and Wear of Rail/Wheel Systems*, Cambridge, 1990, Amsterdam, 1991, pp. 163–178.
- [3]. J. Kalousek, K.L. Johnson, An investigation of short pitch wheel and rail corrugations on Vancouver mass transit system, *Proc. Inst. Mech. Eng.* 206 (F) (1992) 127–135.
- [4]. S.L. Grassie, J. Kalousek, Rail corrugation: characteristics, causes and treatments, *Proc. Inst. Mech. Eng.* 207 (1993) 57–68.
- [5]. S L Grassie. Rail corrugation: characteristics, causes, and treatments. The manuscript was received on 29 November 2008 and was accepted after revision for publication on 20 May 2009. DOI: 10.1243/09544097JRRT264JRRT264. *Proc. IMechE Vol. 223 Part F: J. Rail and Rapid Transit*.
- [6]. Stuart L Grassie. Rail corrugation: advances in measurement, understanding and treatment. *Wear* 258 (2005) 1224–1234.
- [7]. Shaoguang Li, Zili Li, Alfredo Núñez and Rolf Dollevoet. New Insights into the Short Pitch Corrugation Enigma Based on 3D-FE Coupled Dynamic Vehicle-Track Modeling of Frictional Rolling Contact *Appl. Sci.* 2017, 7, 807; doi:10.3390/app7080807.
- [8]. Curt A. Swenson. Locomotive Radial Steering Bogie Experience in Heavy Haul Service. *IHHA'99*. 1999, pp. 79-86.
- [9]. C. Yang, F. Li, Y. Huang, K. Wang, B. He. Comparative study on wheel-rail dynamic interactions of side-frame cross-bracing bogie and sub-frame radial bogie. *J. Mod. Transport.* 21(1)c1-8. DOI 10.1007/s40534-013-0001-3.
- [10]. D.T. Eadie, M. Santoro & W. Powell: Local control of noise and vibration with KELTRACK™ friction modifier and Protector® trackside application: an integrated solution, *Journal of Sound and Vibration*, Vol. 267, Issue 3, October 23, 2003, pp. 761-772.

- [11]. Christophe Collette, MihaitaHorodinca and Andre Preumont. Rotational vibration absorber for the mitigation of rail rutting corrugation. Vehicle System Dynamics Vol. 00, No. 0, Month 2008, 1–19.

IJAETMAS